Spectrochimica Acta Part A: Molecular and Biomolecular Spectroscopy 204 (2018) 696–701

Contents lists available at ScienceDirect

Spectrochimica Acta Part A: Molecular and Biomolecular Spectroscopy

journal homepage: www.elsevier.com/locate/saa

Temperature dependent time resolved mid-IR photoacoustic spectroscopy of a nerve gas simulant DMMP

K.S. Rao [a,c], A.K. Razdan [b], Akansha Tyagi [b], A.K. Chaudhary [a,*]

[a] *Advanced Center of Research in High Energy Materials (ACRHEM), University of Hyderabad, Hyderabad 500046, India*
[b] *Laser Science & Technology Centre (LASTEC), Delhi 110054, India*
[c] *The Guo China-US Photonics Laboratory, Changchun Institute of Optics, Fine Mechanics and Physics, Chinese Academy of Sciences, Changchun, China.*

ARTICLE INFO

Article history:
Received 11 January 2018
Received in revised form 18 May 2018
Accepted 23 June 2018
Available online 30 June 2018

Keywords:
OPO
DMMP
Photoacoustic
Laser
IR-bands

ABSTRACT

The paper reports the temperature dependent pulsed photoacoustic spectroscopy of Dimethyl methylphosphonate (DMMP) a nerve gas simulant between 50 and 180 °C temperature range. The time domain PA spectra are recorded using two mid-IR wavelengths i.e. 3374 nm, 3495 nm of pulse duration 1.5 ns at 1 kHz repetition rate obtained from optical parametric oscillator. Two anti-symmetric stretching vibrational modes of (CH_3P) and (CH_3O) groups of DMMP molecules have very strong vibrational peaks at 2861.2 cm^{-1} (3495 nm) and 2963.8 cm^{-1} (3374 nm), respectively. In addition, we have also recorded the PA spectra of acetone at the vibrational frequency 3115.2 cm^{-1} (3210 nm), which is the strong vibrational mode of CH band. The comparison of two PA spectra of DMMP and acetone recorded using similar PA cavity help us to understand the effect of other functional groups with respect to different excitation wavelengths. The presence of additional acoustic modes in the PA spectra of DMMP (3374 nm) above the boiling point confirms the slow process of thermal decomposition. Finally, the low level detection limit of DMMP in air is of the of the order of 0.91 ppbV.

1. Introduction

There is an urgent need to develope a simple and effective detection technique for chemical and biological warfare agent for military and homeland security [1,2]. Dimethyl methylphosphonate (DMMP) is an organophosphorus compound with the chemical formula $C_3H_9O_3P$ or $CH_3PO(OCH_3)_2$. It is a colourless liquid which can use as a simulant for nerve gas sarin. It has density of the order of 1.145 g/mL, molecular mass 124.08 g/mol, boiling point (B.P.) 181 °C. The detection of DMMP in vapor form requires special type of heating arrangement for the collection of sufficient amount of vapour for the analysis. It has several strong absorption bands between mid-IR and IR range. The strongest IR absorption bands lie between 1464 and 787 cm^{-1} range and covered by CO_2 or QCL laser systems whereas mid-IR range between 2997 and 2365 cm^{-1} is covered by tunable OPO system. We have selected high frequency vibrational modes of anti-symmetric vibrational frequency of CH_3P and CH_3O functional group which lies between 2861.2 and 2963.8 cm^{-1} range, for the recording of photoacoustic (PA) spectra [3].

Pulsed photoacoustic (PA) is well-known technique for trace gas analysis [4,5]. In previous reports, we have demonstrated the improvised design of pulsed photoacoustic pyrolysis technique for identification and understanding of decomposition mechanisms of large number of high energy materials (HEMs). Also, we have established the release of some byproduct gases such as NO_2, N_2O, NO etc. at different temperature using UV–Vis and THz laser system [6,7]. The PA signal generation mechanism varies from the different wavelength range of EM spectra. In case of UV–Vis range, it is attributed to vibronic modes of the molecules whereas, in the terahertz range, the PA signal is generated due to excitation of weak vibrational-rotational lines of the molecules [8–15]. However, in case of mid-IR wavelengths, it is due to vibrational modes of molecules. In the present report, for the first time, we have used the similar type of PA system to understand the thermal stability and decomposition mechanisms of dimethyl methylphosphonate (DMMP) between 30 and 181 °C ranges using the mid infrared wavelengths. The used system has simple vapor collection arrangement and the corresponding vapours are excited with nanoseconds (1.5 ns) pulses obtained from OPO tunable between 2963.8 and 2861.2 cm^{-1} range. Few research groups have reported the PA spectroscopy of DMMP molecules in different spectral range. For example, E.L. Holthoff et al. have reported PA bands of DMMP using QCL laser in CW and pulsed modes between 9.3 and 10 μm range. The recorded absorption peaks are attributed to stretching vibration frequency of $\nu_{(CO)}$. They used N_2 as a carrier gas in the gas generator system which was operated at 100 °C [16,17]. Similarly, Annadi Mukherjee et al. and Sharma et al. have reported the detection of multi-mixture of five numbers of gaseous components such as NH_3, NO_2, acetone, SO_2 and DMMP using QCL laser based PA spectrophotometer where laser was tuned between 6.4 and 9.5 μm

---

[*] Corresponding author.
E-mail addresses: anilphys@yahoo.com akcphys@gmail.com (A.K. Chaudhary).

https://doi.org/10.1016/j.saa.2018.06.089
1386-1425/

range [18–20]. The absorption bands of DMMP are once again attributed to $\nu_{(\mathrm{CO})}$ mode. Since QCL laser based PA spectra are recorded at high repetition rate with broad pulses, therefore, the strength of PA signal lies in µV range. Consequently, recording of the time domain PA spectra in IR region is still a challenging task. However, E. Brunol et al. have demonstrated the use of tin oxide based sensor for the detection of DMMP vapor. They have extracted the vapor of stable DMMP molecules between 300 and 600 °C range and recorded the FTIR and NMR spectra [21,22]. For supply of vapor a special type of electric tension unit was used. Y. Zhang et al. have reported the mid-IR absorption spectra of DMMP vapor in a homemade single pass gas cell using high resolution FTIR. Their study was focused on absorption due to P—C—O and P═O bonds which have strong absorption at 1050.01 and 1275.76 cm^{-1}, respectively [23]. Moreover, nanowire and tubes are also used as a sensor to detect DMMP [24–26]. In this report, we have recorded the thermal PA spectra of DMMP between 30 and 180 °C ranges. In addition, we have also recorded the strong time resolved PA spectra of acetone using the same setup to establish the link between characteristic signature peaks of common CH band present in both the samples. Acetone is a common lab reagent and has signature peaks in UV and IR region. It has polar covalent bonds which are IR active and provide strong absorption spectra between 4000 and 400 cm^{-1} range. There is six C—H stretching modes of acetone but only three are visualized in the IR region. Therefore, we have compared the PA spectra of DMMP with acetone using similar PA cavity at two different excitation wavelengths in the mid-IR range.

2. Experimental Details

The experimental set up for recording of temperature dependent (thermal) fingerprint spectra of liquid DMMP and acetone is shown in the Fig. 2. Optical parametric oscillator (OPO) model - Nano Levante (manufactured by M/S APE, Berlin) generates light in near and mid-IR range was employed for recording of PA signal. It provides short pulses of 1.5 ns duration laser light widely tunable between 1.45 and 1.96 µm (signal) and 2.3 to 4.2 µm (Idler) wavelength range with spectral resolution of 1 nm at 1 kHz repetition rate. It can be internally and externally triggered (TTL), its average signal output power varies from 20 to 40 mW, whereas in idler it varies from 0.5 to 20 mW range. The pulse energy of signal at 1750 nm (signal) was greater than 30 µJ while for idler at 2320 nm wavelength it was greater than 2.5 µJ. The laser beam has TEM$_{00}$ mode.

The PA cell used in the experiment was made of stainless steel. It has an internal diameter of 1.5 cm and length of 7.5 cm and used to record the PA spectrum. The ZnSe windows were placed in both sides of the cell to allow the tunable mid-IR laser radiation. The cell was designed to study the samples in the vapor form therefore, the vapors of DMMP and acetone which is already available in liquid form and can be collected by evacuating the PA cell at room temperature. Since DMMP is a very stable molecule and requires continuous heating under controlled condition. Therefore we have used a round bottom flask which was housed in a temperature controlled oven to convert liquid samples into vapor form 30–181 °C boiling point (B.P.). The 15 mL of liquid sample was placed in a round bottom flask for controlled pyrolysis. A needle valve was used to control the flow rate of vapor through the inlet. The photoacoustic signal (PA signal) produced by vapour was detected by pre-polarized microphones of responsivity 50 mV/Pa (BSWA, China). The microphone was placed in the center of the cell to record the excited resonant cavity modes i.e. longitudinal, radial and azimuthal modes of the cavity in very efficient manner. The output signal of the microphone was fed to the preamplifier which was coupled to the 200 MHz Oscilloscope (Tektronix, U.S.A.) [18]. The fresh vapor of DMMP molecules was allowed into the PA cell to record the temperature dependent PA spectra. Since acetone is a volatile compound at ambient temperature. Therefore, we have evacuated the system, and then allowed the fresh vapor of liquid sample into the PA cell at atmospheric pressure (~600 Torr), for the recording of PA spectra at a maximum output power of excited laser pulses (Fig. 1).

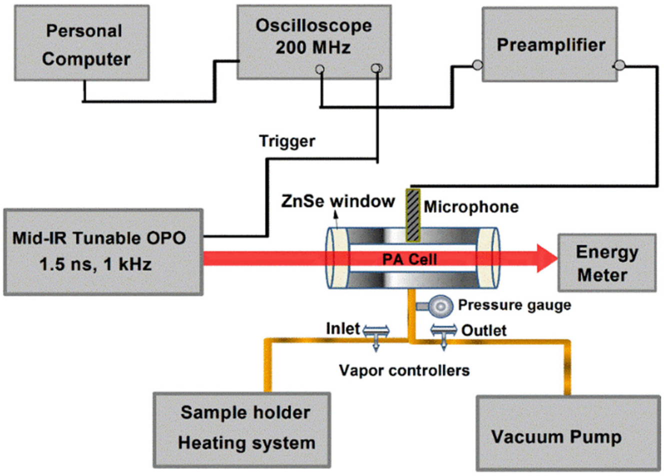

Fig. 1. Experimental setup.

In our previous reports, we have employed the UV–Visible wavelengths i.e. 266 nm and 532 nm of nanoseconds pulses at 10 Hz (100 ms) repetition rate [7,27–30]. In this case, the signal to noise ratio is very high due to the long duration of one pulse to another pulse. However, in the present case, the 1.5 ns duration of mid-infrared laser pulses were operated at repetition rate 1 kHz (these pulses have separation 1 ms only). Therefore, there is a possibility to get the lowest signal to noise ratio. However, due to strong vibrations of DMMP molecules at 2861.2 cm^{-1} and 2963.8 cm^{-1} corresponding to mid-IR wavelengths 3495 and 3374 nm, the considerable signal to noise ratio is achieved with strong separated acoustic modes.

3. Results and Discussion

The experiment was carried out in four steps. In the first step, the liquid DMMP molecules were heated up to its boiling temperature i.e. 180 °C, thereafter the PA spectra were recorded using 3495 and 3374 nm, respectively. In the second step, the PA spectra of DMMP were recorded as a function of temperature at the excitation wavelength 3374 nm. In the third step, using same excitation wavelength at 180 °C, the PA spectra were recorded as a function of data acquisition time and studied the decay behavior of acoustic modes. In the fourth step, the PA spectra of acetone were recorded and compared with the DMMP spectra corresponding to their excitation wavelengths.

3.1. Wavelength-dependent PA Spectra of DMMP

Initially, we have observed the two strong vibrational modes of DMMP in the IR spectra at mid-IR wavelengths [31]. Fig. 2 shows the IR spectra of DMMP, which has two strong vibrations at 2957 cm^{-1} (3374 nm), 2861.2 cm^{-1} (3495 nm). It indicates that the absorbance

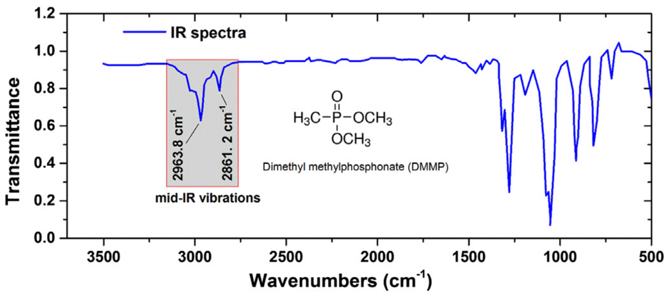

Fig. 2. IR spectra of DMMP [31].

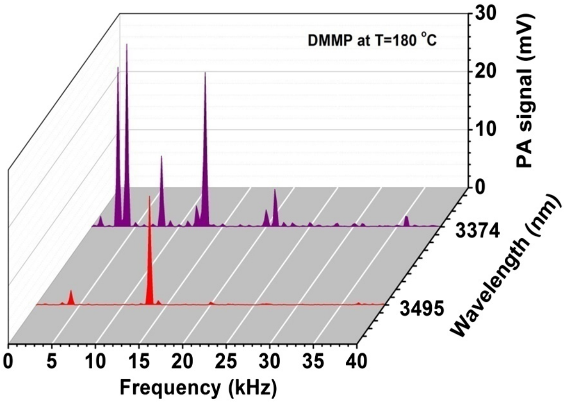

Fig. 3. PA spectra of DMMP as a function of at 3495 and 3374 nm wavelengths.

at 2957 cm^{-1} (3374 nm) is higher than 2861.2 cm^{-1} (3495 nm). Further, we have chosen these two wavelengths to record the PA spectra of DMMP. Fig. 3 shows the PA spectra of DMMP at 3374 and 3495 nm recorded at 180 °C. In case of these two wavelengths, the PA spectra clearly show the excitation of each 1 kHz (i.e. 1, 2, 3…40 kHz) modes, respectively. This is due to higher repetition rate (1 kHz = 1 ms). However, some of the predominant excited modes are matched with the resonance cavity modes of PA cell ($L = 7.5$ cm and $R = 0.75$ cm). The calculated cavity modes (longitudinal (q), radial (n) and azimuthal (m)) are comprised in Table 1, which are measured using the following formulae: $f_{mnq} = \frac{c}{2}\left(\left(\frac{\alpha_{mn}}{R}\right)^2 + \left(\frac{q}{L}\right)^2\right)^{1/2}$, where α_{mn} is the nth zero of the derivative of the mth Bessel function at $r = R$ divided by π, where R and L represent the radius and the length of the cylinder, respectively.

The strength of PA signal and excited acoustic modes are stronger for 3374 nm than 3495 nm. It clearly indicates that DMMP has strong absorption at 3374 nm as compared to the 3495 nm which is also confirmed in FTIR spectra (Fig. 2). In case of PA spectra at 3374 nm, the predominant acoustic modes are present at 3, 4, 8 13, 20, 21 and 36.2 kHz, whereas at 3495 nm the modes are located at 4 and 13 kHz, respectively. Even though the same PA cell geometry has been used but the different acoustic modes are observed with two different absorption bands around 3374 nm and 3495 nm,. The reason is the excitation mechanism and the generation of PA signal vary from wavelength to wavelength. However, the excited modes with two different wavelengths are one of the resonance cavity modes of PA cell as listed in Table 1. It is mentioned that the 3374 nm has strong absorption compared to 3495 nm (is confirmed from both FTIR and PA spectra). Therefore it is possible to get the highest intensity of PA signal with more number of cavity modes at 3374 nm. The modes 4 and 13 kHz are the common excited modes for both excitation wavelengths, which are nearly equivalent to second longitudinal and sixth longitudinal (as well as first radial) modes of PA cavity, respectively. The difference in the acoustic modes and their predominant order as a function of excitation wavelength clearly indicates the variation in the absorption and vibrational mechanisms of two close functional groups.

The vibrational mode at 2957 cm^{-1} (3374 nm), is attributed to mixed antisymmetric vibrational modes of CH_3O and CH_3P whereas the single peak present at 2861.2 cm^{-1} (3495 nm) is due to antisymmetric vibrational mode of CH_3O. This confirms that the contribution of PA signal with the anti-symmetric vibrations for both CH_3O and CH_3P functional groups are higher than the individual antisymmetric vibrations of CH_3O, which is also confirmed in the PA spectra of acetone. In case of 3374 nm, the generated PA signal is resonant of both the functional groups, as a result, the higher strength of PA signal, as well as more number of acoustic modes, is achieved.

Since the intensity of PA signal for 3374 nm is highest. Therefore, in the next section, we have recorded the temperature dependent PA spectra of DMMP to understand its thermal stability and decomposition mechanism at the same wavelength.

3.2. Temperature-dependent PA Spectra of DMMP at 3374 nm

Fig. 4(a, b) shows the PA spectra and behavior of acoustic modes between 30 and 180 °C temperature range. The strength of PA signal increases as a function of temperature. However, at 180 °C the PA spectra has an additional excited mode along with rapid increase in the intensity of 4.5 kHz mode. The acoustic mode present at 13 kHz possessing predominant nature between 30 and 130 °C ranges. However, at 180 °C the modes present at 3 and 4 kHz have higher intensity as compared to 13 kHz. This indicates that the response of lower order longitudinal modes is high at higher concentration of vapor. Whereas between 30 and 130 °C range, the first radial mode (has similar frequency with the sixth longitudinal) has a higher response. This reveals that the change in the vapor density leads to variation in the predominant order of acoustic modes.

The PA spectra also confirm the enhancement of PA signal at 180 °C which is six times higher than the room temperature. It is attributed to the initiation process of thermal decomposition above the boiling point. The dense vapor (like smog) was seen on the wall of the flask (Borosil) at the time of heating. Even after transfer of total vapor to the PA cell by pumping some liquid drops (in condensed form) were seen inside surface of the heating flask (DMMP vapor ionized to liquid). Since 180 °C is the boiling point of this DMMP molecules, as a result, more vapor was produced and leads to generation of strong PA signal. In addition, the acoustic modes present at 3, 4, 8 and 22 kHz as shown in Fig. 3 (b) between 30 and 130 °C temperature ranges are stable in nature. This directly indicates the thermal stability of DMMP within this temperature range.

3.3. Effect of Data Acquisition Time

Fig. 5 shows the PA spectra of DMMP at 180 °C as a function of data acquisition time for the excitation wavelength 3374 nm. The side by side excited modes of PA spectra recorded at 0.25 ms time are overlapped with each other, because, the step-size between the two data points is of the order of 400 Hz. However, for 0.5, 1.0, and 2.5 ms timescales the steps are of the order of 200, 100, and 40 Hz respectively. The PA spectra recorded at 2.5 ms. shows well separated excited modes. It is also interesting to note that the central frequency of acoustic modes does not vary as a function of data acquisition time. The strength of the PA signal and data acquisition times is inversely proportional to each other, i.e. for higher time scales, the intensity of PA signal is lower.

Fig. 6(a, b) shows the exponential decay behavior of 4 and 13 kHz modes of DMMP which belong to two different functional groups. The

Table 1
Calculated frequencies of PA cell ($L = 7.5$ cm, $R = 0.75$ cm) at c = 343 m/s for dry air 20 °C.

Longitudinal (q)	1	2	3	4	5	6	7	8	9	10	11
Modes f (kHz)	2.28	4.57	6.86	9.14	11.43	13.72	16.00	18.29	20.58	22.86	25.15
(q)	12	13	14	15	16	17	18	19	20	21	22
f (kHz)	27.44	29.72	32.01	34.30	36.58	38.87	41.16	43.44	45.73	48.02	50.30
Radial (n) modes	1	2	3	Azimuthal (m) modes	1	2					
f (kHz)	13.4	22.2	30.5	f (kHz)	27.89	38.8					

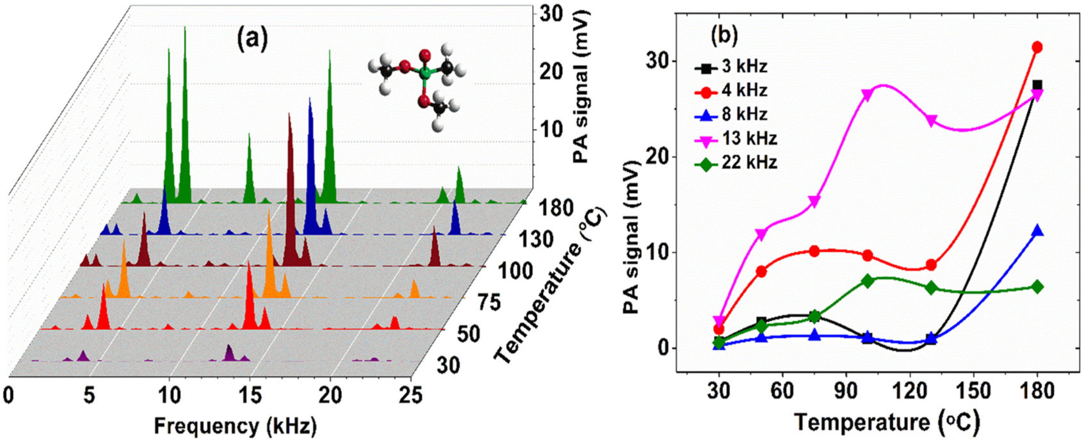

Fig. 4. (a) PA spectra (b) behavior of acoustic modes at 3374 nm, $t = 0.5$ ms with respect to temperature for DMMP.

decay times of 4 and 13 kHz for 3374 are 0.49, 0.55 ms, whereas for 3495 nm are 0.65, 0.27 ms, respectively. In case of $\lambda = 3495$ nm the mode at 4 kHz possesses slow decay time, whereas for 3374 nm it was replaced by 13 kHz. This confirms that accumulation of energy between different acoustic modes with respect to their excitation wavelength. The modes are showing higher decay time revealing that those are prominent ones as compared to other. Also, it is affected by the excitation wavelengths. In our earlier report, we have demonstrated the decay behavior of different cavity modes with excitation of 532 nm in case of NO_2 [27]. The signature (decay behavior) is also seen in case of DMMP, which confirms the generation of an acoustic signal from the sample vapor. The variation in the PA signal with respect to data acquisition time reveals the presence of released vapor. The main purpose of our study based on data aquisition time is to understand the decay behavior of acoustic modes. Finally, It shows the response and presence of vapor released from the DMMP at ambient pressure and 180 °C temperature.

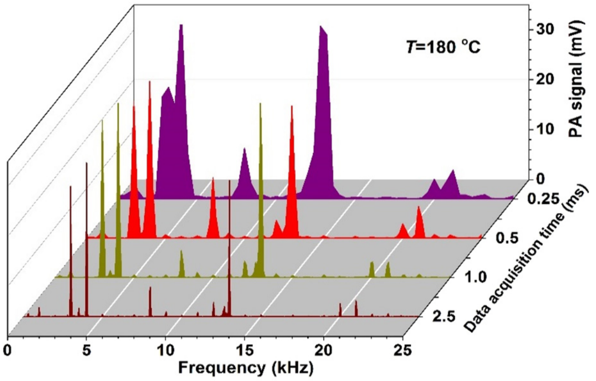

Fig. 5. PA spectra of DMMP as a function of data acquisition time.

3.4. Comparison Between DMMP and Acetone

Fig. 7(a, b) shows the PA spectra of DMMP and acetone recorded at two wavelengths 3374 and 3210 nm respectively at data acquisition time (t) = 0.5 ms. Inset figures show the line-bond structures with different functional groups present in the samples. The excited acoustic modes and their corresponding intensities are listed in Table 2. In that common predominant modes are present at 3 and 4 kHz. In case of DMMP, these modes have the highest intensity than other acoustic modes, whereas for acetone it is occupied by 12 and 18 kHz, respectively. However, all other acoustic modes have different frequencies for both the compounds. For acetone, it has the first predominant mode is present at 12 kHz, whereas it is shifted to 13 kHz for DMMP. In addition, DMMP has strong peaks below 13 kHz frequency range whereas acetone has three numbers of additional acoustic modes with lower intensities within this range. The vibrations from DMMP are observed from CH_3O and CH_3P, whereas for acetone is attributed to C=C—H bond.

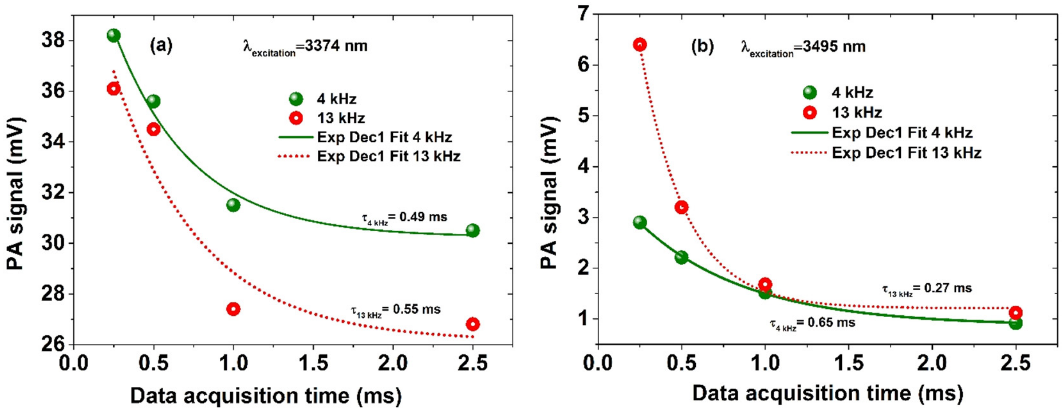

Fig. 6. (a) The decay behavior of acoustic modes with respect to data acquisition time (a) 3374 nm, (b) 3395 nm.

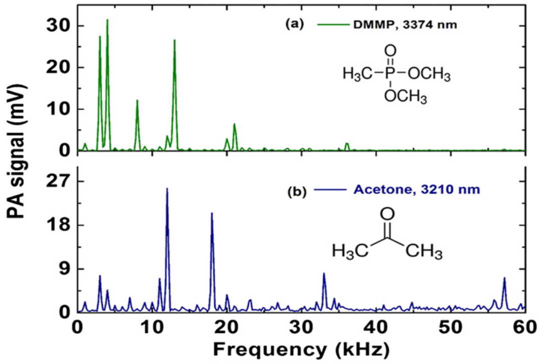

Fig. 7. PA spectra of (a) DMMP at 3374 nm (b) acetone at 3210 nm, $t = 0.5$ ms.

Table 2
Excited acoustic modes and their intensities for both samples.

Sample/wavelength	Acoustic modes frequency *f* (kHz), intensity (I) of PA signal (mV)							
DMMP/3374 nm	*f* (kHz):	3	4	8	13	20	21	36.2
	I (mV):	27.47	31.47	12.18	26.57	2.91	6.44	1.71
Acetone/3210 nm	*f* (kHz):	3	4	11	12	18	33	57.2
	I (mV):	7.62	4.52	7.04	25.56	20.50	8.14	7.21

The excited acoustic modes frequencies are different for DMMP and acetone. Here, we have used two different excitation wavelengths according to sample vibrational modes in the same PA cell. Therefore, the recorded PA spectra can be treated as the signature spectra of the sample at particular excitation wavelength corresponding to given PA cell dimensions.

3.5. Low Limit Detection of PA System

For trace level detection of DMMP vapor in present PA system, we have carefully cleaned the PA system i.e. PA cell and its connecting accessories. Further, the background signal is recorded by filling the cell with air at 600 Torr pressure. After that, we have initiated to find the lowest PA signal at 1 Torr DMMP vapor and buffered with air at 599 Torr, (total vapor pressure 600 Torr) in order to achieve the trace level detection of DMMP vapor inside the PA cell at maximum laser power (0.5–20 mW). In this case, the signal to noise ratio is very weak. This might be due to the low energy of mid-infrared wavelengths (3374 and 3210 nm) and unable to generate the strong PA signal from released vapor at lowest pressure i.e. at 1 Torr, unlike 532 nm excitation wavelength for the low-level detection of NO_2 molecules [32]. However, we measured the low-level detection of our PA system at 5 Torr pressure of DMMP vapor buffered with 595 Torr air for the first radial mode i.e. 13 kHz at excitation wavelength 3374 nm. In this case, the signal to noise ratio (SNR) was quite high and estimated concentration of DMMP molecules was 8334 ppmV. The presence of background noise at 600 Torr air with a maximum intensity was of the order of 0.15 mV (shown in Fig. 8(a)). The maximum intensity of PA signal found to be 1.37 mV (Fig. 8(b)). The signal is 9.13 times higher than the noise for DMMP vapor. The formula for trace level detection of PA system is given by

$$S_{\min} = \frac{\text{Concentration of the sample}}{\text{Signal to Noise Ratio}} = \frac{8334\ \text{ppmV}}{9.13} = 0.91\ \text{ppbV} \qquad (1)$$

Similarly, the trace level detection of acetone is of the order of 0.77 ppbV. It is ascertained c for the acoustic mode 12 kHz at the excitation wavelength 3210 nm. The modes 13 and 12 kHz are one of the predominant modes of the PA spectra of DMMP and acetone corresponding to 3374 and 3210 nm wavelengths, respectively.

4. Conclusions

We have successfully recorded the time domain spectra of DMMP and acetone in the mid-IR region using tunable wavelengths obtained from OPO for the first time. We have also made an attempt to distinguish the effect of each functional group in terms of their PA spectra which also shows the unique signature under similar experimental conditions. The growth of PA signal with respect to temperature highlights the stable nature of DMMP molecules. The comparison of PA spectra of acetone and DMMP also help to understand the behavior of the functional group with respect to their position with other groups. Also, demonstrated the exchange of energy mechanisms in a multimode acoustic cavity which is also link to the vibrational mode of the particular functional group. In addition, we have calculated the trace level detection of vapors of DMMP and acetone for our PA system which is of the order of 0.91 and 0.77 ppbV, respectively.

Acknowledgments

The authors gratefully acknowledge the D.R.D.O. Ministry of Defence, Govt. of India, for financial support to the ACRHEM under phase –III No. ERIP/ER/1501138/M/01/319/D(R&D). We would also like to express our sincere thanks to the Director of LASTEC, DRDO, Delhi and The Director of ACRHEM, University of Hyderabad for extending full support.

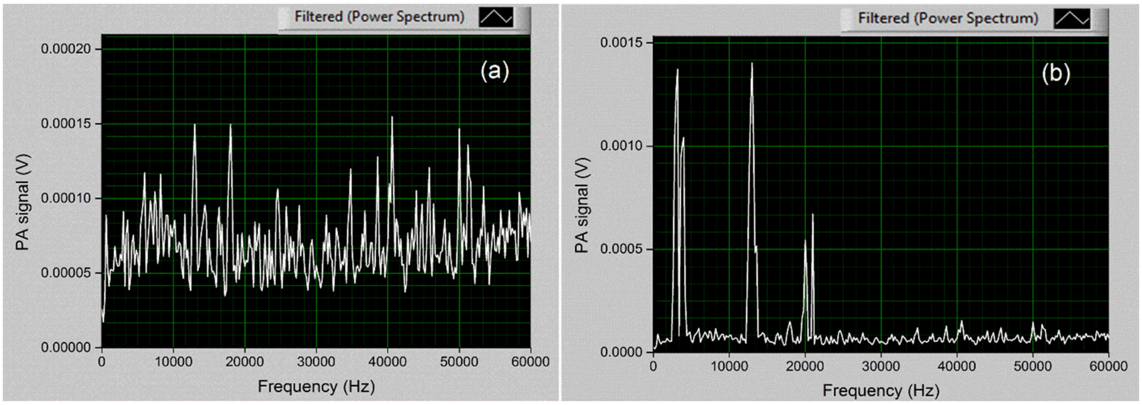

Fig. 8. (a) Background noise signal of PA system, and (b) at 5 Torr DMMP vapor +595 Torr air at data acquisition time $t = 0.5$ ms.

References

[1] The Guardian Head Lines9th April, 2017.

[2] Guide for the selection of chemical detection equipment for emergency first responders, Guide 100-06, 3rd editonU.S. Department of Homeland Security, January 2007.

[3] D.A. Panayotov, J.R. Morris, Thermal decomposition of a chemical warfare agent simulant (DMMP) on TiO_2: adsorbate reactions with lattice oxygen as studied by infrared spectroscopy, J. Phys.Chem. C. 113 (2009) 15684–15691.

[4] A. Miklós, P. Hess, Á. Mohácsi, J. Sneider, S. Kamm, S. Schäfer, Improved photoacoustic detector for monitoring polar molecules such as ammonia with a 1.53 μm DFB diode laser, AIP Conf. Proc. 463 (1999) 1–4.

[5] M.B. Filho, M.G. Silva, M.S. Sthel, D.U. Schramm, H. Vargas, A. Miklós, P. Hess, Ammonia detection by using quantum-cascade laser photoacoustic spectroscopy, Appl. Opt. 45 (2006) 4966–4971.

[6] Konda Srinivasa Rao, A.K. Chaudhary, Development of UV–Vis-THz laser based pulsed photoacoustic pyrolysis technique for the study of thermal decomposition, Stability Mechanisms of High Energy Materials, ILA, Kiran, 2017.

[7] K.S. Rao, A.K. Chaudhary, F. Yehya, A.S. Kumar, Study of acoustic fingerprinting of nitromethane and some triazole derivatives using UV 266 nm pulsed photoacoustic pyrolysis technique, Spectrochim. Acta Part A Mol. Biomol. Spectrosc. 147 (2015) 316–323, https://doi.org/10.1016/j.saa.2015.03.017.

[8] G.D. Gillispie, A.U. Khan, The electronic structure of NO_2. II. The 2B2 ← 2A1 and 2B1 ← 2A1 absorption systems, J. Chem. Phys. 65 (1976) 1624–1633, https://doi.org/10.1063/1.433306.

[9] J. Kalkman, H.W. Van Kesteren, Relaxation effects and high sensitivity photoacoustic detection of NO_2 with a blue laser diode, Appl. Phys. B Lasers Opt. 90 (2008) 197–200, https://doi.org/10.1007/s00340-007-2895-0.

[10] Y.Q. Guo, A. Bhattacharya, E.R. Bernstein, Photodissociation dynamics of nitromethane at 226 and 271 nm at both nanosecond and femtosecond time scales, J. Phys. Chem. A 113 (2009) 85–96, https://doi.org/10.1021/jp806230p.

[11] J.F. Arenas, J.C. Otero, D. Peláez, J. Soto, The ground and excited state potential energy surfaces of nitromethane related to its dissociation dynamics after excitation at 193 nm, J. Chem. Phys. 119 (2003) 7814, https://doi.org/10.1063/1.1600436.

[12] S. Zabarnick, J.W. Fleming, A.P. Baronavski, Production of OH from the collision-free photodissociation of nitromethane at 266 nm, J. Chem. Phys. 85 (1986) 3395, https://doi.org/10.1063/1.450961.

[13] L.J. Butler, D. Krajnovich, Y.T. Lee, G.S. Ondrey, R. Bersohn, The photodissociation of nitromethane at 193 nm, J. Chem. Phys. 79 (1983) 1708, https://doi.org/10.1063/1.446015.

[14] E.D. Palik, K.N. Rao, Pure rotational spectra of CO, NO, and N_2O between 100 and 600 microns, J. Chem. Phys. 25 (1956) 1174–1176, https://doi.org/10.1063/1.1743172.

[15] D.M. Mittleman, R.H. Jacobsen, R. Neelamani, R.G. Baraniuk, M.C. Nuss, Gas sensing using terahertz time-domain spectroscopy, Appl. Phys. B Lasers Opt. 67 (1998) 379–390, https://doi.org/10.1007/s003400050520.

[16] E.L. Holthoff, D.A. Heaps, P.M. Pellegrino, Development of a MEMS-scale photoacoustic chemical sensor using a quantum cascade laser, IEEE Sensors J. 10 (2010) 572–577.

[17] E. Holthoff, J. Bender, P. Pellegrino, A. Fisher, Quantum cascade laser-based photoacoustic spectroscopy for trace vapor detection and molecular discrimination, Sensors 10 (2010) 1986–2002, https://doi.org/10.3390/s100301986.

[18] D.A. Heaps, P. Pellegrino, Investigations of intraband quantum cascade laser source for a MEMS-scale photoacoustic sensor, Proc SPIE 2007, p. 65540F , (1–9).

[19] A. Mukherjee, M. Prasanna, M. Lane, R. Go, I. Dunayevskiy, A. Tsekoun, C.K.N. Patel, Optically multiplexed multi-gas detection using quantum cascade laser photoacoustic spectroscopy, Appl. Opt. 47 (2008) 1–4.

[20] R.C. Sharma, S. Gupta, K. Deepak, G. Sanchit, H. Chandra, Standoff quantum cascade laser photoacoustic spectroscopy based explosive detection system, J. Lasers Opt. Photonics 1 (2014) 1–8, https://doi.org/10.4172/2469-410X.1000109.

[21] E. Brunol, F. Berger, M. Fromm, R. Planade, Detection of dimethyl methylphosphonate (DMMP) by tin dioxide-based gas sensor: response curve and understanding of the reactional mechanism, Sensors Actuators B Chem. 120 (2006) 35–41, https://doi.org/10.1016/j.snb.2006.01.040.

[22] I.N. Smirnova, A. Cuisset, F. Hindle, G. Mouret, R. Bocquet, O. Pirali, P. Roy, A.V.M. Schumann, M.V.L.V.M. State, Gas-phase synchrotron FTIR spectroscopy of weakly volatile alkyl phosphonate and alkyl phosphate compounds: vibrational and conformational analysis in the terahertz/far-IR spectral domain, J. Phys. Chem. B 114 (2010) 16936–16947.

[23] R.D. Suenram, F.J. Lovas, D.F. Plusquellic, A. Lesarri, Y. Kawashima, J.O. Jensen, A.C. Samuels, Fourier transform microwave spectrum and ab initio study of dimethyl methylphosphonate, J. Mol. Spectrosc. 118 (2002) 110–118, https://doi.org/10.1006/jmsp.2001.8486.

[24] D. Kumar, P. Jha, A. Chouksey, J.S.B.S. Rawat, R.P. Tandon, P.K. Chaudhury, 4-(Hexafluoro-2-hydroxy isopropyl) aniline functionalized highly sensitive flexible SWCNT sensor for detection of nerve agent simulant dimethyl methylphosphonate, Mater. Chem. Phys. 181 (2016) 487–494, https://doi.org/10.1016/j.matchemphys.2016.06.085.

[25] Z. Pei, P. Ding, W. Zhang, Z. Luo, G. Li, M. Engineering, C. Learning, R. Holloway, Study of a QCM dimethyl methylphosphonate sensor based on a ZnO-modified nanowire-structured manganese dioxide film, Sensors 10 (2010) 8275–8290, https://doi.org/10.3390/s100908275.

[26] T. Zhang, S. Mubeen, N.V. Myung, , Recent progress in carbon nanotube-based Nanotechnology 19 (2008), 332001. https://doi.org/10.1088/0957-4484/19/33/332001.

[27] K.S. Rao, F. Yehya, A.K. Chaudhary, A.S. Kumar, A.K. Sahoo, Thermal stability study of nitro-rich triazole derivatives using temperature dependent time resolved pulsed photoacoustic (PA) technique, J. Anal. Appl. Pyrolysis 109 (2014) 132–139, https://doi.org/10.1016/j.jaap.2014.07.002.

[28] K.S. Rao, A.K. Chaudhary, Study of thermal stability and acoustic fingerprint spectra of phenyl and benzyl triazole derivatives using time resolved pulsed photoacoustic pyro analysis technique, Thermochim. Acta 614 (2015) 149–156, https://doi.org/10.1016/j.tca.2015.06.020.

[29] K.S. Rao, A.K. Chaudhary, Investigation of thermal decomposition and stability of energetic 1, 2, 4-triazole derivatives using UV laser based pulsed photoacoustic technique, RSC Adv. 6 (2016) 47646–47654, https://doi.org/10.1039/C6RA06773E.

[30] K.S. Rao, A.K. Chaudhary, N. Kommu, A.K. Sahoo, Evaluation of thermal stability and acoustic fingerprint spectra of energetic 1,2,4-triazoles based on bond lengths of chemical substituents using pulsed photoacoustic technique, RSC Adv. 6 (2016) 4053–4062, https://doi.org/10.1039/C5RA21369J.

[31] http://webbook.nist.gov/cgi/cbook.cgi?ID=C756796&Type=IR-SPEC&Index=0#IR-SPEC.

[32] F. Yehya, A.K. Chaudhary, Study of damping, saturation and surface losses on low level detection of NO_2 using time resolved pulsed photo acoustic technique, Opt. Commun. 312 (2014) 16–22, https://doi.org/10.1016/j.optcom.2013.08.052.